Uniform ALD deposition of Pt nanoparticles within 1D anodic TiO_2 nanotubes for photocatalytic H_2 generation

JeongEun Yoo[a], Raul Zazpe[b], Gihoon Cha[a], Jan Prikryl[b], Imgon Hwang[a], Jan M. Macak[b] and Patrik Schmuki[a,c]*

[a] Department of Materials Science, Institute for Surface Science and Corrosion WW4-LKO, Friedrich-Alexander University, Martensstraße 7, D-91058 Erlangen, Germany;
[b] Center of Materials and Nanotechnologies, Faculty of Chemical Technology, University of Pardubice, Nam. Cs. Legii 565, 530 02 Pardubice, Czech Republic;
[c] Chemistry Department, Faculty of Sciences, King Abdulaziz University, 80203 Jeddah, Saudi Arabia Kingdom

* Corresponding author: E-mail:schmuki@ww.uni-erlangen.de

Abstract

In the present work we investigate the utilization of Pt nanoparticles produced by atomic layer deposition (ALD) within anodic TiO_2 nanotube (NT) layers for photocatalytic H_2 production. By varying numbers of ALD cycles, Pt nanoparticles with different diameters, uniformly decorating the tube walls were produced. The Pt nanoparticle size (2-15 nm), the Pt mass loading and areal density were strongly dependent on the number of Pt ALD cycles. The deposited Pt nanoparticles turned out to be highly effective as co-catalyst for photocatalytic H_2 generation. A most effective performance for solar light photocatalysis was reached after 26 ALD cycles (yielding an optimal areal coverage with particles of a diameter ≈ 7 nm). For UV light optimum photocatalytic efficiency was reached after 40 ALD cycles.

Keywords: TiO_2 nanotubes; Platinum; Photocatalysis; H_2 evolution; Atomic Layer Deposition

Introduction

Since the pioneering work of Fujishima and Honda in 1972, the production of H_2 by photocatalytic splitting of H_2O on semiconductors has been extensively investigated [1]. Among the different studied photocatalysts, titanium dioxide (TiO_2) received wide attention mainly due to a suitable conduction and valence band edge position for photogenerated charge carriers reacting with water as well as for its nontoxicity and stability against photocorrosion [2]. The TiO_2 conduction band edge lies higher than the redox potential of water (-0.45 and 0 V vs. NHE, respectively, at pH 0) [3]. Therefore, it is possible to reduce H_2O to H_2 by photoexcited electrons that cross the TiO_2 band gap ($Eg_{TiO_2} \approx 3.0 – 3.2$ eV) [4,5].

However, pristine TiO_2 shows low efficiencies for H_2 production and a kinetically slow electron transfer to reactants. Nanostructured photocatalysts can be employed in order to improve the electron transfer efficiency. Particularly one dimensional (1D) nanostructures, such as anodic TiO_2 nanotubes (NTs), have attracted significant attention in the last decade in photocatalysis and photoelectrochemistry as the growth conditions can be easily adjusted leading to a large palette of nanotubular geometries [6–12]. 1D TiO_2 structures can promote directional charge transport and orthogonal electron-hole separation and thus enhance photocatalytic reaction rates [13]. However, except for nanostructuring to reach reasonable H_2 evolution from TiO_2 photocatalysts, cocatalysts used to be decorated. These co-catalysts aid charge separation and transfer; most typical are noble metal nanoparticles (such as Au, Pd and Pt) [14,15].

Among them Pt is the most efficient co-catalyst for the H_2 generation reaction. Pt nanoparticles at the TiO_2 surface can enable efficient electron transfer at the catalyst/environment interface by providing a favorable solid state junction to TiO_2, and additionally catalyze the hydrogen recombination reaction ($2H^0 \rightarrow H_2$) [16].

In the case of TiO_2 NT layers, different Pt decoration methods have been described– the most frequently used techniques are various wet chemical routes, photo-deposition methods, and conventional sputter deposition techniques onto the NT layer [16–19]. However, these techniques lead commonly to a non-homogeneous particle distribution, in general a higher loading at the tube mouth takes place and a depletion of deposition deeper in the tube. This mouth accumulation effect becomes increasingly severe, the higher the aspect ratio of the nanotube layers [20,21].

In recent years atomic layer deposition (ALD) has become a prime method for deposition of a wide number of materials such as oxides, sulfides and metals among others [22–24]. In addition, it is one of the few methods enabling a homogeneous and conformal secondary material deposition into high aspect ratio structures [25]. The effective utilization of ALD for deposition of various materials within TiO_2 nanotube layers has been demonstrated e.g. for oxides [26–30] and sulfides [31,32], yielding interesting synergic effects. Even though the use of the ALD to deposit Pt nanoparticles on various catalytic supports has been reported in previous works [33–35], no reports show an effective deposition of Pt nanoparticles within high aspect ratio 1D TiO_2 tubular nanostuctures.

In the present work we investigate for the first time the deposition of Pt nanoparticles by ALD within TiO_2 nanotube layers, and evaluate the effect of the Pt decoration on photocatalytic H_2 evolution under deep UV irradiation and under solar light irradiation.

Experimental

Self-ordered vertically-aligned TiO_2 nanotube layers were grown by anodization of Ti metal foils (0.125 mm thick, 99.5 % purity). Ti foils were cleaned by sonication in acetone, ethanol and deionized water (15 min for each step), and then dried in a N_2 stream.

The anodization of the Ti layers was performed in a two-electrode electrochemical O-ring cell (O-ring diameter of 10 mm) with a Pt plate as cathode. The electrolyte was composed of 1.5 M lactic acid (LA, 90 %, Sigma-Aldrich), 0.1 M ammonium fluoride (NH_4F, 98 %, Sigma-Aldrich) and 5 wt. % of DI water in ethylene glycol (EG, 99.5 %, Sigma-Aldrich) [36]. The anodization experiments were performed under potentiostatic conditions, using 120 V from a high-voltage potentiostat (Jaissle IMP 88 PC) for an anodization time of 10 min. After anodization, samples were sonicated to remove the nanotubular layer and a dimpled structure was left on the Ti substrate, leading to more ordered TiO_2 nanotubes in the subsequent second anodization. The second anodization was carried out under the same conditions (electrolyte, voltage).

Single-walled TiO_2 nanotubes can be obtained from as-grown TiO_2 nanotubes by following procedure; the as-grown samples obtained after anodization were annealed at 150 ˚C for 1 h in air atmosphere, with a heating and cooling rate of $30^{\circ}Cmin^{-1}$ using a rapid thermal annealer (Jipelec JetFirst100). Afterwards, the annealed nanotubes were etched by piranha solution (1:3 vol. % of H_2O_2:H_2SO_4) at 110 ˚C for 70 sec [37]. The as-formed single walled TiO_2 nanotubes were crystallized by annealing at 450°C, for 1 h, in air atmosphere, using a rapid thermal annealer, with a heating and cooling rate of 30°C min^{-1}. Reference flat TiO_2 layers were prepared by thermal annealing of identical Ti substrates (450°C, 1h, air).

Afterwards, Pt nanoparticles were deposited into TiO_2 nanotube layers and reference flat layers using atomic layer deposition tool (thermal ALD, TFS 200, Beneq) and various numbers of deposition cycles: 8, 16, 24, 26, 28, 40, 48, 72. (Trimethyl)-methyl-cyclopentadienyl-platinum(IV) (Strem, elec. grade, 99%, heated up to $80^{o}C$ to obtain a proper vapor pressure) and oxygen (Messer, 99.95%) were used as Pt precursor and oxidizing agent, respectively. One ALD deposition cycle was defined by the following sequence: Pt pulse (1 s)-N_2 purge (5 s)-O_2 pulse

(1.5 s)-N_2 purge (5 s). The deposition temperature was 300 ^oC using N_2 (99.9999 %) as carrier and purging gas at a flow rate of 400 standard cubic centimeters per minute (sccm) for both purposes.

For the morphological characterization of the Pt-decorated TiO_2 nanotube layers, a field-emission scanning electron microscope (Hitachi, FE-SEM, S4800) and a transmission electron microscope (Philips, CM30) were used. Images from these microscopes were used to evaluate the average Pt nanoparticle diameter. In parallel, SEM images taken from the reference flat layers were used to extract a measure for the areal particle density. X-ray diffraction analysis (XRD, X'pert Philips MPD with a Panalytical X'celerator detector) using graphite monochromized CuKα radiation (wavelength 1.54056 Å) was performed for determining the crystalline structure of the samples. Their composition and the chemical state were characterized using X-ray photoelectron spectroscopy (XPS, PHI 5600, US) and peak positions were calibrated with respect to the Ti2p peak at 458 eV. Energy-dispersive X-ray spectroscopy (EDAX, Genesis, fitted to SEM chamber) was also used for the chemical analysis of the samples.

For the photocatalytic H_2 generation experiments, the samples were immersed into 20 vol% ethanol-water solutions within a sealed quartz tube. The ethanol-water solution (volume ~ 7 mL) and the cell head-space (volume ~ 8 mL) were purged with N_2 gas for 20 min prior to photocatalysis.

Two different light sources were used for the photocatalytic experiments: *i)* a CW-laser emitting UV light (I_0 = 60 mW cm^{-2}, λ = 325 nm), and *ii)* an AM 1.5 solar simulator (300 W Xe, I_0 = 155 mW cm^{-2}, light spot size ~ 20 cm^2, Solarlight) calibrated to 100 $mWcm^{-2}$. In order to determine the amount of generated H_2, the gas that evolved under irradiation was accumulated within the headspace of the quartz reactor and was then analyzed by gas chromatography (using a

GCMS-QO2010SE chromatograph, Shimadzu) withdrawing 200 µL samples with a gas tight syringe.

For total reflectance measurements, a Lambda 950 UV/Vis spectrometer (Perkin Elmer) was employed in a range of 800-200 nm using an integrating sphere. The irradiated beam size was 0.785 cm^2, and interval of wavelength step was 2 nm. As a background reference, a white-flat reference was used.

Results and discussion

TiO_2 NT layers were produced as described in the experimental section. Figs 1a, b show SEM images of a typical layer grown to a thickness of 7 µm, after a treatment to obtain a single wall structure and after annealing at 450˚C in air to crystalize the tubes [37,38]. The SEM images show these tubes, to have a diameter of ≈ 100 nm, and to be uniformly single walled from top to bottom (Figs. 1a, b).

The TiO_2 nanotube layers were then decorated with Pt nanoparticles using ALD by applying different number of cycles, as described in the experimental section. The ALD process shows a nucleation delay and following and growth mechanism of Pt in line with previous reports [33–35]. That is nucleation delay during the initial ALD cycles of noble metals occurs and has been reported to be due to the lack of adsorption sites [39,40] and/or large differences in the surface energy between substrate and noble metal [41,42]. Figs 1c~h give representative SEM and TEM images of the Pt nanoparticles loaded within TiO_2 nanotube layers and they clearly show presence of Pt nanoparticles even at their bottom (deepest) parts (Figs. 1f and h). These images

confirm the capability of ALD to deposit Pt particles into high aspect ratio tubes in a homogeneous and conformal fashion [26–30].

A detailed inspection of Pt nanoparticles produced by different number of ALD cycles was carried out within TiO_2 nanotube layers. First Pt clusters (detectable by TEM) formed using 20 ALD cycles. Figs. 1c, d depicts corresponding TEM images, from which small Pt nanoparticles (average diameter ~ 2 nm) can be seen. After this initial growth, Pt nanoparticle decoration becomes visible also by SEM. Figs.1e ~ h show SEM cross-sections of TiO_2 NT after 40 and 72 cycles. The corresponding average particle diameter increased to 11 and 15 nm, respectively. The same growth trend was also observed on reference flat TiO_2 layers.

Fig. 2a shows the size distribution of Pt nanoparticles within TiO_2 nanotubes which was evaluated from SEM images by statistical analysis. As it can be seen, with increasing number of ALD cycles the average Pt nanoparticle size increases. The particles are however, not entirely monodisperse in size, as revealed by standard deviation displayed via error bars. However, this size distribution is well in line with the mass increase obtained from EDX as shown in Fig. 2b. Additional EDX data shown in Fig. 2c represent a semiquantitative measure for the average Pt mass loading as with an increasing Pt loading also the information depth of EDX decreases (typically for un-loaded TiO_2 nanotube layers the EDX information depth is around 5-10 µm) [43]. Nevertheless the trend of a dramatic increase in Pt mass loading after first 20 cycles is evident and further confirmed by the XRD data in Fig. 2d and XPS data in Fig. 2e. In accord, the areal density of particles evaluated on flat layers shows a significant increase between 16 and 24 cycles (inset of Fig. 2a). This flat layer results suggest coalesce to occur in the range of 26 cycles. This pattern is qualitative in line with the trend observed on the TiO_2 nanotubes.

XRD patterns obtained for TiO_2 nanotube layers before and after Pt ALD process (Fig. 2d) confirmed anatase structure, indicating that ALD process did not affect the TiO_2 nanotube crystallinity. For higher Pt ALD cycles (40 and 72), Pt peaks can be identified, while the anatase peaks and the Ti metal peak became increasingly attenuated due to the lower penetration depth of X-rays resulting from an increased mass density (due to the increased Pt content).

Fig. 2e shows the composition of the blank and Pt-loaded TiO_2 nanotube layers. From the XPS HR spectra of the Pt4f peak in inset of Fig. 2e it can be seen that the ALD Pt films consists of metallic Pt (*i.e.*, Pt_0), and no - contribution of adsorbed oxygen or Pt oxides can be detected. This oxide-free state is important in view of the activity of Pt in photocatalysis [16]. The small content of fluorine is due to F-ion uptake during the electrochemical growth of the tubes in the NH_4F electrolyte [44].

For the photocatalytic H_2 generation experiments, Pt free and Pt loaded TiO_2 nanotube layers were examined in a 20 vol% EtOH solution under AM 1.5 (100 $mWcm^{-2}$) conditions and under plain UV conditions (He-Cd laser 325 nm, 60 $mWcm^{-2}$).

Fig 3a shows the H_2 generation as a function of the Pt ALD cycles for 7 μm thick TiO_2 nanotube layers for the different illumination conditions. As expected the ALD deposited Pt nanoparticles act as efficient co-catalyst for H_2 evolution. An optimum Pt size for solar light was revealed for 26 cycles (~7 nm) while for 325 nm light the maximum occurred for 40 cycles (~ 11 nm). The occurrence of these maxima can be attributed to the light penetration depth, i.e. the competition between the positive effect of loading of Pt nanoparticles (leading to a higher co-catalytic efficiency) and the negative effect that is shading of the TiO_2 surface. These activation maxima are observed for a different Pt nanoparticle loading for solar light and plain UV light.

This can be ascribed to the different light absorption characteristics of Pt-decorated TiO_2 nanotube layers at different wavelengths.

Fig. 3b shows the total reflectance of the TiO_2 nanotube layers decorated with Pt nanoparticles obtained with a various umber of Pt ALD cycles. With increasing cycle number (and according Pt nanoparticle diameter and areal density) particularly the visible light absorption and super-bandgap-light close to the band gap (3.2eV, approx. 390 nm of wavelength) are strongly affected for 26 ALD cycles [45]. From the data in Fig. 3b, it is clear that the 325 nm light is absorbed in a much shorter tube depth than solar light with a high intensity close to Eg = 3.2 eV (390 nm). Therefore, a lower particle loading is required for an optimum performance than for UV light.

These findings illustrate that there are several important factors that affect the performance of TiO_2 nanotube layers decorated by Pt nanoparticles using ALD. Most importantly, for the different light source (wavelength) different optima in Pt particle size exist. In addition, the presented findings show the advantageous use of ALD for decoration of nanotubular layers. That is due to the specific island like growth of nanoparticles, it is possible to control the particles size and density. Other technique do not allow for the purpose of hydrogen generation to decorate high aspect ratio nanotubular or nanoporous structures with a similar degree of control.

In summary the present results demonstrate that ALD is very efficient technique for a dense and homogenous decoration of TiO_2 nanotube layers by Pt nanoparticles of different size, mass and areal density. In addition, these particles show very good performance for photocatalytic H_2 produced on the 1D nanotubular catalyst support. The best performance was achieved for particles with the size of approx. 7 (corresponds to 26 cycles and highest areal density of particles) and 11 nm (corresponds to 40 cycles), respectively, depending on the light irradiation source (AM 1.5 solar simulator or UV laser, respectively). The presented results pave a way for uniform

and efficient noble metal decoration of various 1D nanotube layers with high aspect ratio for various catalytic applications.

Acknowledgements

The authors would like to acknowledge the European Research Council, the DFG, the DFG "Engineering of Advanced Materials" cluster of excellence and Ministry of Youth Education and Sports of the Czech Republic (projects nr. LM2015082, CZ.02.1.01/0.0/0.0/16_013/0001829) for financial support.

References

[1] A. Fujishima, K. Honda, Electrochemical photolysis of water at a semiconductor electrode, Nature. 238 (1972) 37–38.

[2] K. Lee, A. Mazare, P. Schmuki, One-dimensional titanium dioxide nanomaterials: nanotubes, Chem. Rev. 114 (2014) 9385–454.

[3] A. Fujishima, T.N. Rao, D. a. Tryk, Titanium dioxide photocatalysis, J. Photochem. Photobiol. C Photochem. Rev. 1 (2000) 1–21.

[4] I. Paramasivam, H. Jha, N. Liu, P. Schmuki, A review of photocatalysis using self-organized TiO_2 nanotubes and other ordered oxide nanostructures, Small. (2012) 3073–3103.

[5] K. Lee, R. Hahn, M. Altomare, E. Selli, P. Schmuki, Intrinsic Au decoration of growing TiO_2 nanotubes and formation of a high-efficiency photocatalyst for H_2 production, Adv. Mater. 25 (2013) 6133–6137.

[6] P. Roy, S. Berger, P. Schmuki, TiO_2 nanotubes: synthesis and applications, Angew. Chem. Int. Ed. 50 (2011) 2904–2939.

[7] N.T. Nguyen, S. Ozkan, I. Hwang, A. Mazare, P. Schmuki, TiO_2 nanotubes with laterally spaced ordering enable optimized hierarchical structures with significantly enhanced photocatalytic H_2 generation, Nanoscale. 8 (2016) 16868–16873.

[8] N.T. Nguyen, M. Altomare, J.E. Yoo, N. Taccardi, P. Schmuki, Noble metals on anodic TiO_2 nanotube mouths: thermal dewetting of minimal Pt co-catalyst loading leads to significantly enhanced photocatalytic H_2 generation, Adv. Energy Mater. 27 (2015) 3208-3215.

[9] J.M. Macak, M. Zlamal, J. Krysa, P. Schmuki, Self-organized TiO_2 nanotube layers as highly efficient photocatalysts, Small. 3 (2007) 300–304.

[10] S. Bauer, S. Kleber, P. Schmuki, TiO_2 nanotubes: tailoring the geometry in H_3PO_4/HF electrolytes, Electrochem. Commun. 8 (2006) 1321–1325.

[11] J.M. Macak, P. Schmuki, Anodic growth of self-organized anodic TiO_2 nanotubes in viscous electrolytes, Electrochim. Acta. 52 (2006) 1258–1264.

[12] S.P. Albu, A. Ghicov, J.M. Macak, P. Schmuki, 250 μm long anodic TiO_2 nanotubes with hexagonal self-ordering, Phys. Status Solidi - Rapid Res. Lett. 1 (2007) 65–67.

[13] Z. Miao, D. Xu, J. Ouyang, G. Guo, X. Zhao, Y. Tang, Electrochemically induced sol-gel preparation of single-crystalline TiO_2 nanowires, Nano Lett. 2 (2002) 717–720.

[14] I. Paramasivam, J.M. Macak, P. Schmuki, Photocatalytic activity of TiO_2 nanotube layers loaded with Ag and Au nanoparticles, Electrochem. Commun. 10 (2008) 71–75.

[15] Z. Zhang, Z. Wang, S.W. Cao, C. Xue, Au/Pt nanoparticle-decorated TiO_2 nanofibers with plasmon-enhanced photocatalytic activities for solar-to-fuel conversion, J. Phys. Chem. C. 117 (2013) 25939–25947.

[16] J. Yoo, M. Altomare, M. Mokhtar, A. a. Alshehri, S. A. Al-Thabaiti, A. Mazare, P. Schmuki, Photocatalytic H_2 generation using dewetted Pt-decorated TiO_2 nanotubes – optimized dewetting and oxide crystallization by a multiple annealing process, J. Phys. Chem. C.120 (2016) 15884–15892.

[17] J. Kiwi, M. Grätzel, Optimization of conditions for photochemical water cleavage. aqueous Pt/TiO_2 (anatase) dispersions under ultraviolet light, J. Phys. Chem. 88 (1984) 1302–1307.

[18] Z.-D. Gao, Y.-F. Qu, X. Zhou, L. Wang, Y.-Y. Song, P. Schmuki, Pt-decorated g-C_3N_4/TiO_2 nanotube arrays with enhanced visible-light photocatalytic activity for H_2 evolution, Chem. Open. 5 (2016) 197–200.

[19] J.M. Macak, P.J. Barczuk, H. Tsuchiya, M.Z. Nowakowska, A. Ghicov, M. Chojak, S. Bauer, S. Virtanen, P.J. Kulesza, P. Schmuki, Self-organized nanotubular TiO_2 matrix as support for dispersed Pt/Ru nanoparticles: enhancement of the electrocatalytic oxidation of methanol, Electrochem. Commun. 7 (2005) 1417–1422.

[20] J.E. Yoo, K. Lee, P. Schmuki, Dewetted Au films form a highly active photocatalytic system on TiO_2 nanotube-stumps, Electrochem. Commun. 34 (2013) 351–355.

[21] J.E. Yoo, M. Altomare, M. Mokhtar, A. Alshehri, S. A. Al-Thabaiti, A. Mazare, P. Schmuki, Anodic TiO_2 nanotube arrays directly grown on quartz glass used in front- and back-side irradiation configuration for photocatalytic H_2 generation, Phys. Status Solidi Appl. Mater. Sci. 213 (2016) 2733–2740.

[22] R.W. Johnson, A. Hultqvist, S.F. Bent, A brief review of atomic layer deposition: From fundamentals to applications, Mater. Today. 17 (2014) 236–246.

[23] N.P. Dasgupta, X. Meng, J.W. Elam, A.B.F. Martinson, Atomic layer deposition of metal sulfide materials, Acc. Chem. Res. 48 (2015) 341–348.

[24] B.S. Lim, A. Rahtu, R.G. Gordon, Atomic layer deposition of transition metals, Nat. Mater. 2 (2003) 749–754.

[25] J.W. Elam, D. Routkevitch, P.P. Mardilovich, S.M. George, Conformal coating on ultrahigh-aspect-ratio nanopores of anodic alumina by atomic layer deposition, Chem. Mater. 15 (2003) 3507–3517.

[26] J. Tupala, M. Kemell, E. Härkönen, M. Ritala, M. Leskelä, Preparation of regularly structured nanotubular TiO_2 thin films on ITO and their modification with thin ALD-grown layers, Nanotechnology. 23 (2012) 125707.

[27] I. Turkevych, S. Kosar, Y. Pihosh, K. Mawatari, T. Kitamori, J. Ye, K. Shimamura, Synergistic effect between TiO_2 and ubiquitous metal oxides on photocatalytic activity of composite nanostructures, Nippon Seramikkusu Kyokai Gakujutsu Ronbunshi/Journal Ceram. Soc. Japan. 122 (2014) 393–397.

[28] J.M. Macak, J. Prikryl, H. Sopha, L. Strizik, Antireflection ln_2O_3 coatings of self-organized TiO_2 nanotube layers prepared by atomic layer deposition, Phys. Status Solidi - Rapid Res. Lett. 9 (2015) 516–520.

[29] R. Zazpe, M. Knaut, H. Sopha, L. Hromadko, M. Albert, J. Prikryl, V. Gärtnerová, J.W. Bartha, J.M. Macak, Atomic layer deposition for coating of high aspect ratio TiO_2 nanotube layers, Langmuir. 32 (2016) 10551–10558.

[30] H. Sopha, M. Krbal, S. Ng, J. Prikryl, R. Zazpe, F.K. Yam, J.M. Macak, Highly efficient photoelectrochemical and photocatalytic anodic TiO_2 nanotube layers with additional TiO_2 coating, Appl. Mater. Today. 9 (2017) 104–110.

[31] S.K. Sarkar, J.Y. Kim, D.N. Goldstein, N.R. Neale, K. Zhu, C.M. Elliott, A.J. Frank, S.M. George, In_2S_3 atomic layer deposition and its application as a sensitizer on TiO_2 nanotube arrays for solar energy conversion, J. Phys. Chem. C. 114 (2010) 8032–8039.

[32] M. Krbal, J. Prikryl, R. Zazpe, H. Sopha, J.M. Macak, CdS-coated TiO_2 nanotube layers: downscaling tube diameter towards efficient heterostructured photoelectrochemical conversion, Nanoscale. 9 (2017) 7755–7759.

[33] L. Baker, A. S. Cavanagh, D. Seghete, S.M. George, A. J.M. MacKus, W.M.M. Kessels, Z.Y. Liu, F.T. Wagner, Nucleation and growth of Pt atomic layer deposition on Al_2O_3 substrates using (methylcyclopentadienyl)-trimethyl platinum and O_2 plasma, J. Appl. Phys. 109 (2011) 84333.

[34] Y. Zhou, D.M. King, X. Liang, J. Li, A.W. Weimer, Optimal preparation of Pt/TiO_2 photocatalysts using atomic layer deposition, Appl. Catal. B Environ. 101 (2010) 54–60.

[35] N.P. Dasgupta, C. Liu, S. Andrews, F.B. Prinz, P. Yang, Atomic layer deposition of platinum catalysts on nanowire surfaces for photoelectrochemical water reduction, J. Am. Chem. Soc. 135 (2013) 12932–12935.

[36] S. So, K. Lee, P. Schmuki, Ultrafast growth of highly ordered anodic TiO_2 nanotubes in lactic acid electrolytes, J. Am. Chem. Soc. 134 (2012) 11316–11318.

[37] S. So, I. Hwang, P. Schmuki, Hierarchical DSSC structures based on “single walled” TiO_2 nanotube arrays reach a back-side illumination solar light conversion efficiency of 8%, Energy Environ. Sci. 8 (2015) 849–854.

[38] I. Hwang, S. So, M. Mokhtar, A. Alshehri, S. A. Al-Thabaiti, A. Mazare, P. Schmuki, Single-walled TiO_2 nanotubes: enhanced carrier-transport properties by $TiCl_4$ treatment, Chem. A Eur. J. 21 (2015) 9204–9208.

[39] H-B-R. Lee, M.N. Mullings, X. Jiang, B.M. Clemens, S.F. Bent, Nucleation-controlled growth of nanoparticles by atomic layer deposition, Chem. Mater. 24 (2012) 4051-4059.

[40] H-B-R. Lee, S.H. Baeck, T.F. Jaramillo, S.F. Bent, Growth of Pt nanowires by atomic layer deposition on highly ordered pyrolytic graphite, Nano Lett. 13 (2013) 457-463.

[41] C.T. Campbell, Ultrathin metal films and particles on oxide surfaces: structural, electronic and chemisorptive properties, Surf. Sci. Rep. 27 (1997) 1–111

[42] L. Baker, A.S. Cavanagh, J. Yin, S.M. George, A. Konghanand, F.T. Wagner, Growth of continuous and ultrathin platinum films on tungsten adhesion layers using atomic layer deposition techniques, Appl. Phys. Lett. 101 (2012) 111601

[43] A. Wassilkowska, A. Czaplicka-Kotas, A. Bielski, M. Zielina, An analysis of the elemental composition of micro-samples using EDS technique, Tech. Trans. Chem. 2014 (2015) 133-148.

[44] J.M. Macak, S. Aldabergerova, A. Ghicov, P. Schmuki, Smooth anodic TiO_2 nanotubes: Annealing and structure, Phys. Status Solidi Appl. Mater. Sci. 203 (2006) 67–69.

[45] G. Cha, P. Schmuki, M. Altomare, Free standing membranes to study the optical properties of anodic TiO_2 nanotube layers, Chem. An Asian J. 11 (2016) 789–797.

Figure captions

Fig .1

SEM and TEM images show anodic single-walled TiO_2 nanotube layers. (a) and (b) are pristine tubes, (e)-(h) are ALD treated ((e) and (f) after 40 cycles; (g) and (h) after 72 cycles). (c) and (d) TEM images of single-walled TiO_2 NT layers after 20 cycles.

Fig .2

(a) The size of ALD Pt nanoparticles as a function of ALD cycles on TiO_2 NTs and on flat surfaces (inset). (b) and (f) Pt contents on the ALD treated samples (b) by EDX; (f) by XPS. (c) EDX spectra; (d) XRD pattern; (e) XPS spectrum of TiO_2/ALD-Pt samples.

Fig .3

(a) Photocatalytic H_2 generation as a function of Pt-ALD loading cycles under UV light (left) and solar light (right). (b) Total reflectance spectra of anodic single-walled TiO_2 NTs with and without Pt ALD layers.

Figure 1

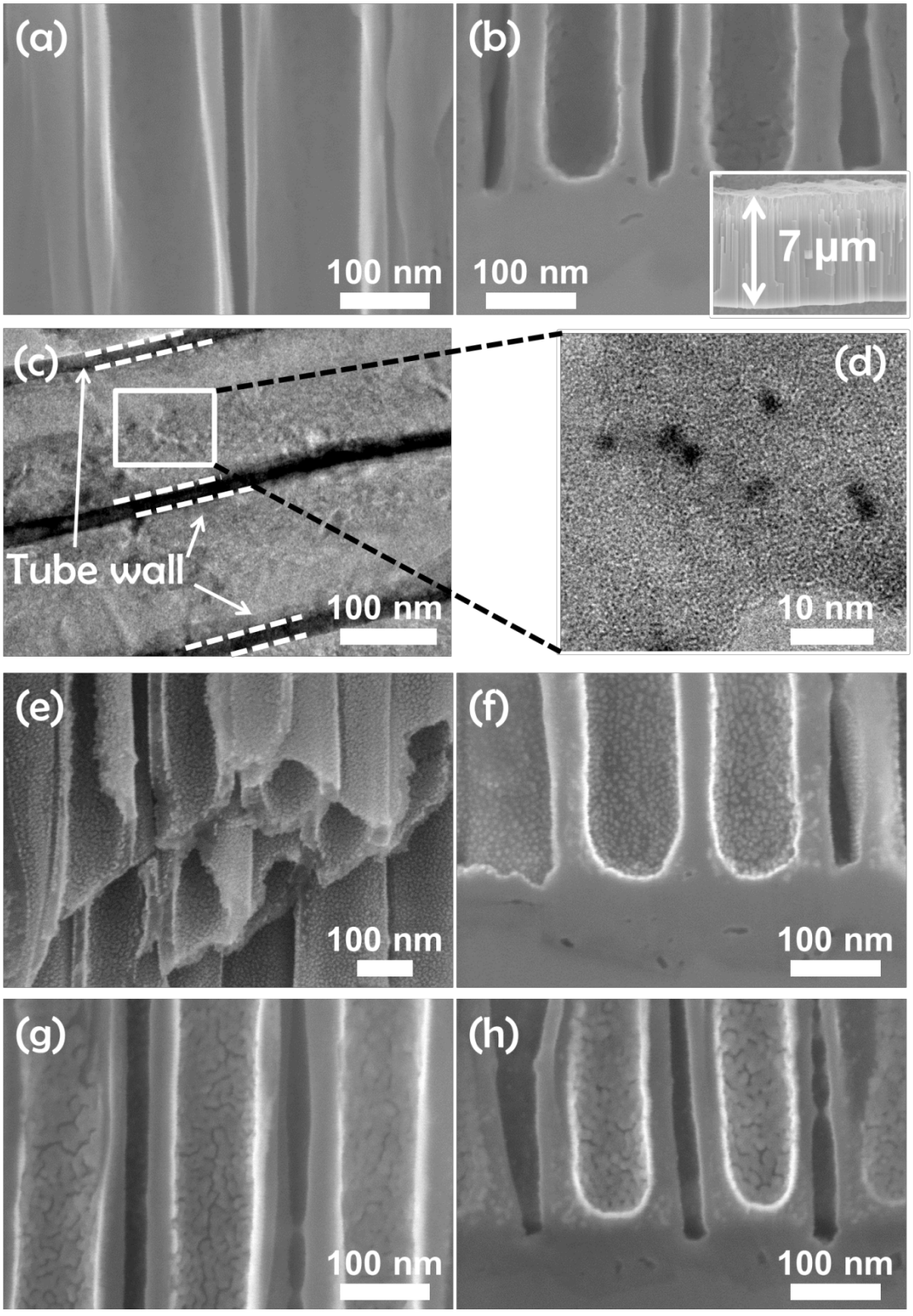
(a)
100 nm
(b)
100 nm
7 μm
(c)
Tube wall
100 nm
(d)
10 nm
(e)
100 nm
(f)
100 nm
(g)
100 nm
(h)
100 nm

Figure 2

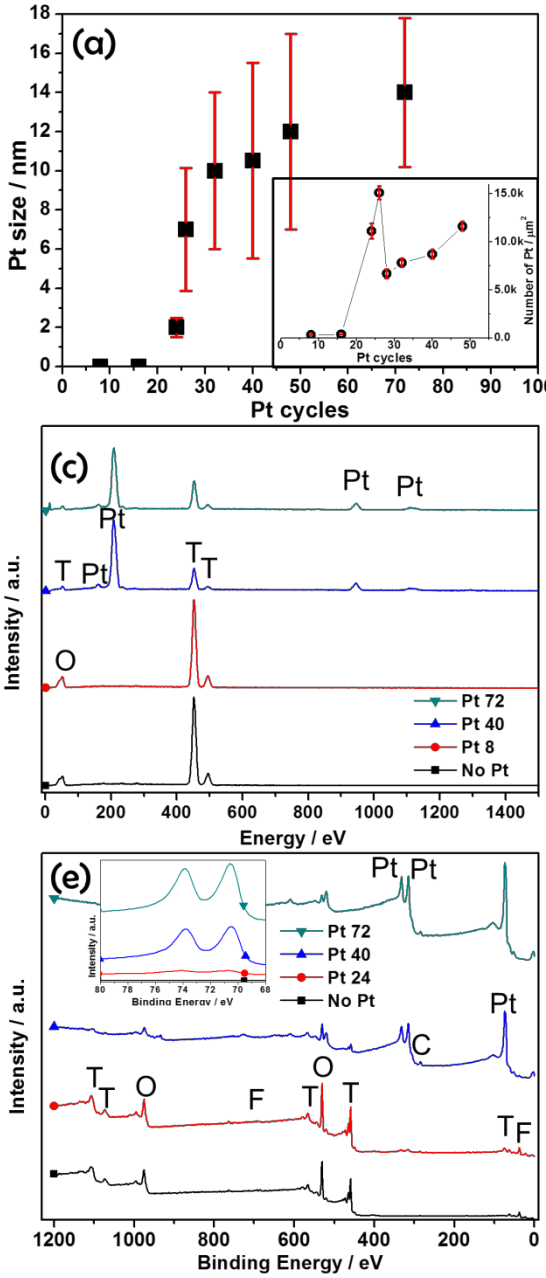

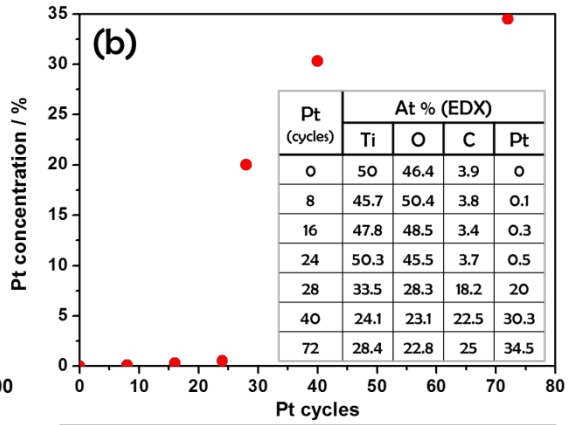

Pt (cycles)	At % (EDX)			
	Ti	O	C	Pt
0	50	46.4	3.9	0
8	45.7	50.4	3.8	0.1
16	47.8	48.5	3.4	0.3
24	50.3	45.5	3.7	0.5
28	33.5	28.3	18.2	20
40	24.1	23.1	22.5	30.3
72	28.4	22.8	25	34.5

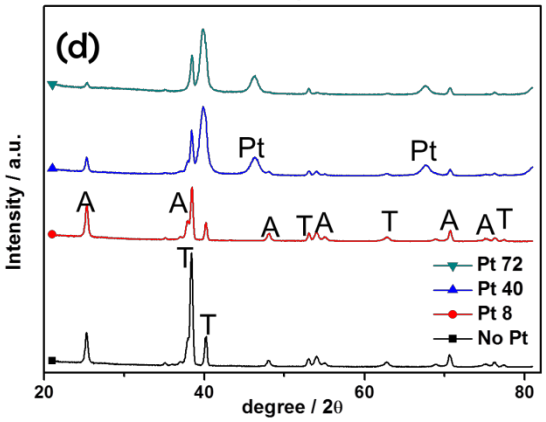

(f)

Pt (cycles)	At % (XPS)				
	Ti	O	C	Pt	F
0	26.4	71.2	1.1	0	1.3
8	28	69.7	2.7	0	1.9
24	26.3	67.0	4.5	1.2	1.0
40	8.1	38.0	25.5	28.2	0.2
72	1.0	20.3	29.1	49.6	0

Figure 3

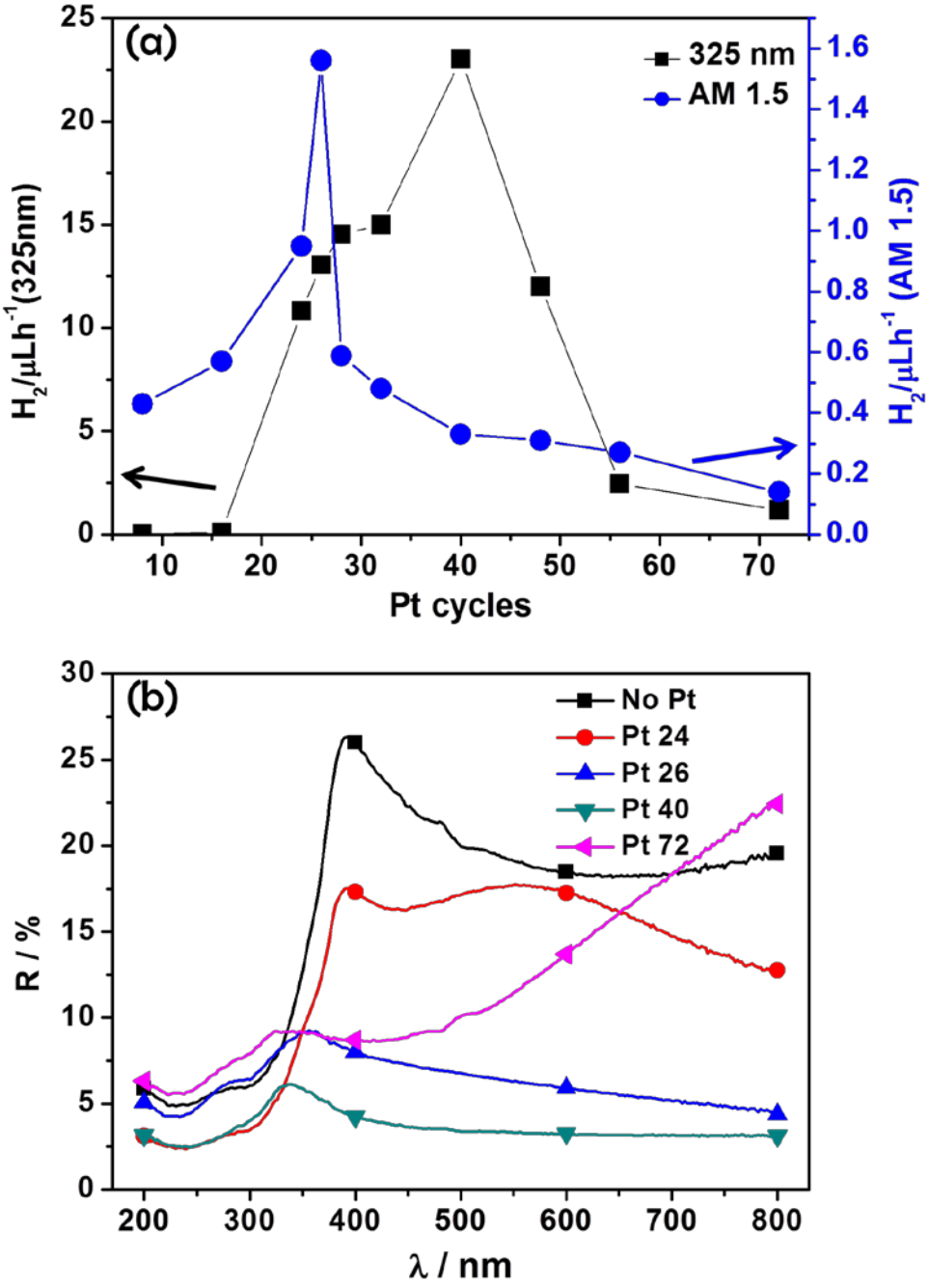
(a)
325 nm
AM 1.5
H2/μLh-1(325nm)
H2/μLh-1 (AM 1.5)
Pt cycles
(b)
No Pt
Pt 24
Pt 26
Pt 40
Pt 72
R / %
λ / nm